Recrystallization and grain growth in single tungsten fiber-reinforced tungsten composites

Wartacz, D. A. H.; Riesch, J.; Pantleon, K.; Pantleon, W.

Published in:
Journal of Physics: Conference Series

Link to article, DOI:
10.1088/1742-6596/2635/1/012034

Publication date:
2023

Document Version
Publisher's PDF, also known as Version of record

Recrystallization and grain growth in single tungsten fiber-reinforced tungsten composites

Recrystallization and grain growth in single tungsten fiber-reinforced tungsten composites

D A H Wartacz[1], J Riesch[2], K Pantleon[1] and W Pantleon[1]

[1] Technical University of Denmark, 2800 Kongens Lyngby, Denmark.
[2] Max-Planck-Institute for Plasma Physics, 85748 Garching, Germany.

E-mail: dahwa@dtu.dk

Abstract. High heat fluxes in future fusion reactors pose big challenges on the materials of plasma-facing components due to restoration processes occurring at high temperatures. Tungsten is considered most suitable as plasma-facing material. To overcome its inherent brittleness at low temperatures, tungsten fiber-reinforced tungsten composites are developed which contain ductile, potassium-doped, drawn tungsten wires in an undeformed tungsten matrix. Such composites show pseudo-ductile behavior, an improved toughness and a more controlled fracture compared to undeformed tungsten. Model systems containing a single fiber either without any interlayer or with an yttria interlayer between fiber and matrix are annealed and characterized by electron backscatter diffraction (EBSD) in order to investigate their thermal stability. The restoration process in wire and matrix differ from each other: Recrystallization followed by grain growth occurs in the deformation structure of the wire. Grain growth is the sole mechanism affecting the undeformed matrix. An yttria interlayer between fiber and matrix is supposed to separate the differently restoring microstructures from each other and thereby preserve the improved mechanical properties of the composite. The investigation focuses on characterizing the as-processed condition and the microstructural changes after annealing at 1450 °C for either four days or two weeks. After two weeks of annealing, grains in the region or the vicinity of the wire have coarsened so much that former fiber and matrix cannot be distinguished any longer; not even in a model composite with a 1 μm thick yttria interlayer.

1. Introduction

Energy systems of the future depend upon development of advanced materials. In particular, the requirements for materials for plasma-facing components in fusion reactors are extraordinarily demanding and tungsten is considered as the only suitable material. Tungsten has the highest melting point of all metals, shows high thermal conductivity, has good strength and creep resistance at elevated temperatures [1] as required for materials for plasma-facing components [2]. The biggest drawback for the usage of tungsten is its inherent brittleness at low temperature similar to any other body-centered cubic metal. Tungsten fiber-reinforced tungsten composites (W_f/W) overcome the intrinsic brittleness of tungsten by utilizing extrinsic toughening mechanisms resulting in a pseudo-ductile behavior [3–5]. W_f/W composites consist of drawn tungsten wires as fibers (W_f), which are ductile at room temperature [6], in an undeformed tungsten matrix (W). Two different routes for producing such composites are currently being deployed, either chemical vapour deposition of tungsten on tungsten wires [7] or powder metallurgical routes where mixtures of tungsten wires with tungsten powders are consolidated by sintering [8].

During operation of fusion reactors, materials of plasma-facing components will be exposed to high heat fluxes. Restoration processes occurring in the material under these conditions can be detrimental for the mechanical properties. For instance, the pseudo-ductile behavior of W_f/W composites roots in the ductility of the tungsten wires achieved by their deformation structure as well as their capability to debond and being pulled-out from matrix. If the wire recrystallizes and the matrix grains coarsen at the high operation temperatures, potential intergrowth between both constituents will eliminate the interface between them and the otherwise improved mechanical properties will be lost.

The materials investigated in the presented work are cylindrical model W_f/W composites where a tungsten matrix is chemically vapor-deposited on a single tungsten wire as fiber. To investigate the microstructural evolution and a potential breakdown of the interface, high temperature annealing is performed followed by microstructural characterization by means of electron backscatter diffraction (EBSD). Single fiber composites with and without an yttria interlayer are annealed at 1450 °C for various periods of time.

2. Material and methods

2.1. Material

Different types of single fiber composites are manufactured specifically for this investigation: either without any interlayer between the fiber and the matrix or with a 1 μm thick yttria interlayer between both (results on composites with a thicker yttria interlayer of 3 μm manufactured simultaneously are not included here). Drawn tungsten wires with a diameter of 150 μm and doped with 60 ppm of potassium were acquired from OSRAM GmbH. The drawn wires were wound around a steel frame to realize two rows of seven free-standing straight wires each. In this configuration, yttria layers of the desired thickness are deposited directly on selected wires by reactive magnetron sputtering while covering all others with an aluminium foil. Due to geometrical restrictions, magnetron sputtering is performed in two steps at the Max-Planck-Institute of Plasma Physics, Garching, Germany. After deposition of an yttria layer with desired thickness on one side of the wires, the frame is turned by 180° to deposit yttria on the other side as well. After magnetron sputtering a thick layer of tungsten is chemically vapor deposited using a dedicated setup at Forschungszentrum Jülich, Germany. Further on, this CVD layer of tungsten is referred to as matrix. Cylindrical rods with a length of about 40 mm are produced (as sketched in figure 2.2a). After CVD, the outer diameters of these single fiber composites are between 2.5 mm and 3.7 mm depending on the distance of the wire from the gas inlet; close to the inlet the layer thickness tends to be thinner than further away.

2.2. Experimental procedure

The obtained rods are hot-embedded for extra support during cutting. Discs with a thickness of 1.3 mm or 0.5 mm are cut from the rods with an Accutom-50 from Struers. For annealing at high temperatures, specimens are encapsulated in quartz glass ampules to prevent oxidation. The ampules are evacuated, flushed with Argon, evacuated again and finally sealed with a blowtorch. The ampules are put in a pre-heated tube furnace NaberTherm RHTH 50-150/18, removed after annealing at 1450 °C for 4 days or 2 weeks and cooled to room temperature by air-cooling.

For microstructural characterization, the top surfaces of the disc-shaped samples are ground with SiC paper up to 4000 grit size, polished with a 3 μm diamond suspension and finally electropolished for approximately 7 seconds in a 3% NaOH suspension with a voltage of 12 V and a current around 2 A. Such an electropolished surface constituting a cross section of a cylindrical specimen with an Y_2O_3 interlayer of 1 μm thickness is shown in figure 2.2b.

Orientation data are gathered on the prepeared surfaces (cross sections of the composite) by EBSD with an accelerating voltage of 20 kV and different steps sizes. Two different

scanning electron microscopes (SEMs) were used, a Zeiss Supra SEM with an Oxford Instruments Nordlys3 EBSD detector and a Zeiss Sigma SEM using a Cnano EBSD detector from Oxford instruments. All orientation maps are presented as collected without any filtering or removal of unindexed points. High angle boundaries (HABs) with disorientation angles above 15° are indicated in black, low angle boundaries (LABs) with disorientation angles between 2° and 15° in white. The data are analyzed using the Matlab plugin toolbox MTEX Version 5.8.1 [11] and evaluated further by own purposely developed routines.

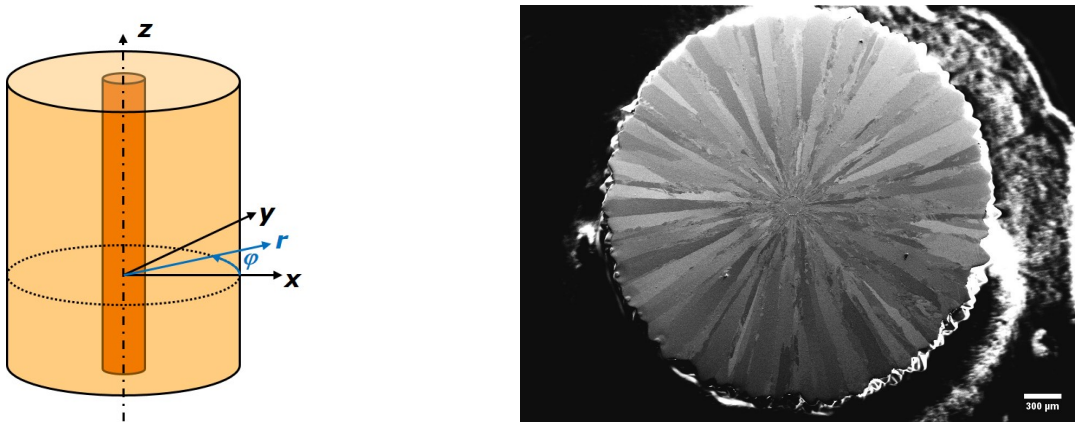

(a) (b)

Figure 1. Single fiber W_f/W composites: a) Sketch of a model composite with the coordinate systems used: A cross section of the rod is indicated by the dashed line. b) Secondary electron image of a cross section of a W_f/W composite with a 1 μm thick Y_2O_3 interlayer.

3. Results and discussion

3.1. As-processed state — single fiber composite with 1 µm thick yttria interlayer

Overview orientation maps from a model composite with (thin) yttria interlayer in its as-processed state are presented in figure 2. Due to the large step size of 5 μm chosen to acquire a map of the entire cross section, neither orientations in the wire, nor in the interlayer are acquired. All three orientation maps clearly reveal the microstructure of the matrix with large columnar grains having grown radially outwards during CVD, confirming the impression from figure 2.2a. This is similar to what has been observed previously in single fiber composites with and without oxide interlayers [9, 10]. Even the same peculiar spatial arrangement of orientations can be recognized from the colors: Horizontally elongated grains appear red when the crystallographic direction along the x-axis is shown, indicating a preference for having a $\langle 100 \rangle$ direction along their growth direction. Similarly, vertically elongated grains turn red when indicating the crystallographic direction along the y-axis revealing the same preference for a $\langle 100 \rangle$ direction. Consequently, both orientation maps in figure 2a and b evidence a preference of columnar growth along a $\langle 100 \rangle$ direction during CVD; more precisely, wedge-shaped grains grow predominantly along one of their $\langle 100 \rangle$ directions from the vicinity of the interlayer outwards.

In order to establish the preferential growth direction unambiguously, an evaluation procedure has been developed [10] taking into account the more appropriate cylindrical coordinate system. As marked in blue in figure 2.2a, the radial direction r of a cylindrical coordinate system points in a cross section outwards from the origin and the azimuthal direction φ along the perimeter. The crystallographic direction along this radial direction can be highlighted in orientation maps by adjusting the Euler angle φ_1 describing the orientation at each pixel individually according to its azimuthal angle φ in the map (note that in [10] erroneously φ_2 is mentioned). The

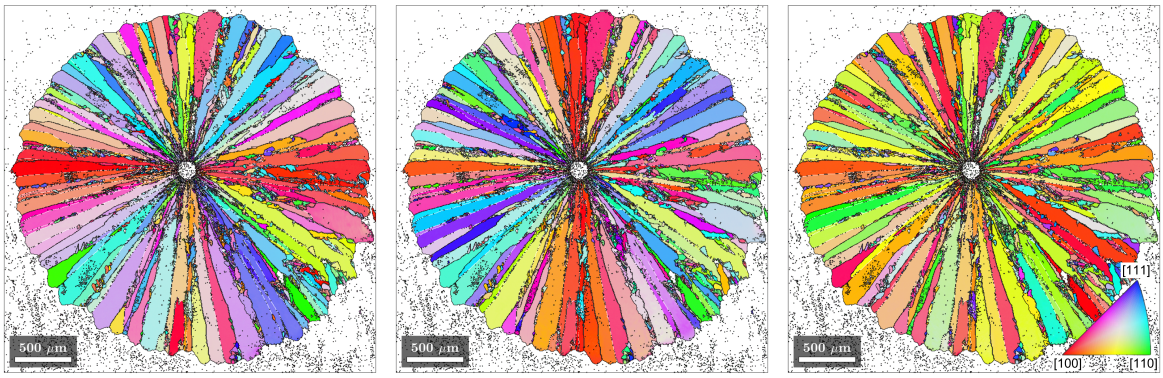

(a) (b) (c)

Figure 2. Orientation maps of the cross section of a single tungsten fiber-reinforced tungsten composite with a 1 μm thick yttria interlayer in the as-processed state. The colors reflect the crystallographic directions along different sample directions according to the inset: (a) along x-, (b) along y- and (c) along z-direction. HABs are indicated in black, LABs in white.

resulting orientation map highlighting the crystallographic direction along the radial direction in figure 3.1 appears almost entirely red confirming the preferred alignment of ⟨100⟩ directions with the radial direction and hence the existence of a cyclic ⟨100⟩ ring fiber texture. (The occasionally occurring cyan color indicates a radial alignment of ⟨221⟩ directions and results from twinning during deposition, cf. [12].)

The existence of a cyclic ring fiber texture (cf. [13] for texture classification) is confirmed by the pole figures with respect to the cylindrical coordinate system provided in figure 4a. The 100 pole figure shows a high pole density along the radial direction and rotational symmetry around that; the 110 pole figure substantiates the latter. An ideal ⟨100⟩ fiber texture along the radial direction in the cylindrical coordinate system translates to a cyclic ⟨100⟩ ring fiber texture in Cartesian coordinates [10]. Quantification of the strength of the cyclic ⟨100⟩ ring fiber texture by analyzing the individual orientations reveals a volume fraction of 89 % when allowing a maximal inclination angle of 15° between the radial and the closest ⟨100⟩ direction. (Twins forming a cyclic ⟨221⟩ ring fiber texture account for another 9 % of the volume.)

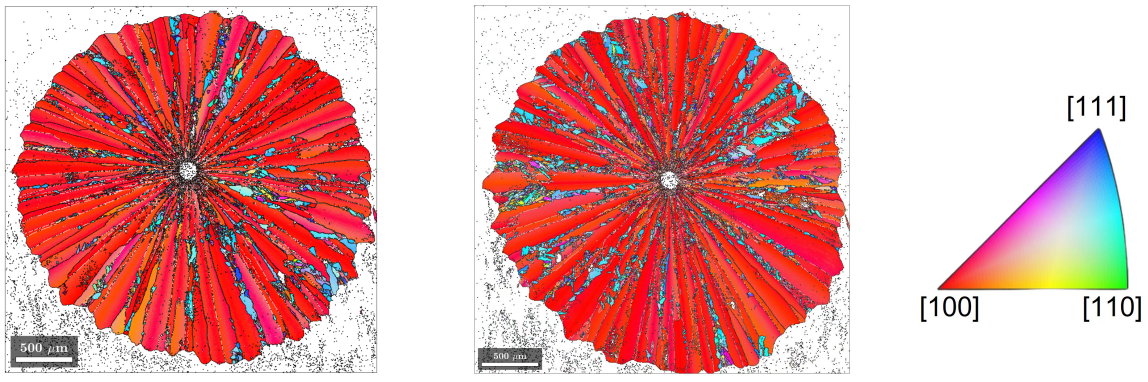

(a) (b)

Figure 3. Orientation maps of the cross sections of single tungsten fiber-reinforced tungsten composites in the as-processed state: a) with a 1 μm thick yttria interlayer and b) without an interlayer. The colors reflect the crystallographic directions along the radial direction defined in figure 2.2a according to the inverse pole figure on the left hand side.

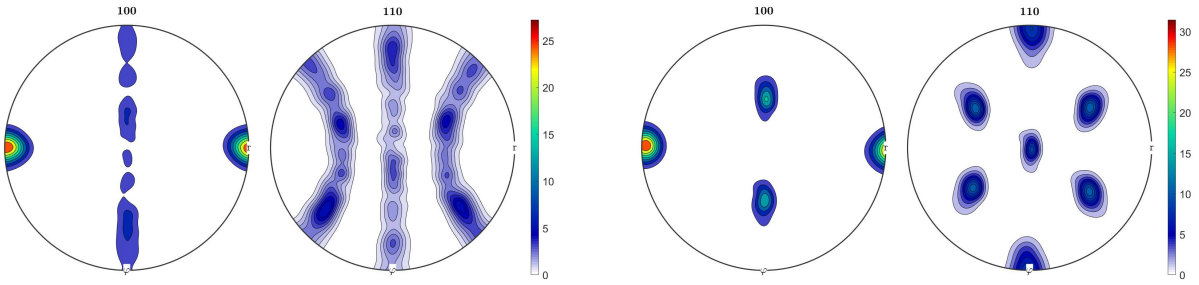

(a) (b)

Figure 4. 100 and 110 pole figures obtained from orientation data gathered on cross sections of single tungsten fiber-reinforced tungsten composites in the as-processed state: a) with a 1 μm yttria interlayer and b) without an interlayer. Pole densities are presented with respect to the local radial, azimuthal and axial directions (r,φ,z) in stereographic projection.

3.2. As-processed state — single fiber composite without interlayer

Orientation maps of a cross section of a model composite without interlayer in its as-processed state are presented in figure 5. The overview maps display the same columnar microstructure along the radial direction as the model composite with yttria interlayer, but with a pronounced difference in coloring revealing a quite different texture within the matrix. In particular, the orientation map in figure 5c appears dominantly green indicating a strong alignment of $\langle 110 \rangle$ directions with the z-axis. The red colors of the horizontally and vertically elongated grains when coloring with respect to the x- and y-direction, respectively, hint towards the same preferred alignment of $\langle 100 \rangle$ with the growth direction as in the model composite with yttria interlayer. Applying the same procedure of adjusting the Euler angle φ_1 pixel by pixel for changing to a cylindrical coordinate system, turns the orientation map presenting the directions along the radial direction in figure 3.1b dominantly red. As seen from the pole figures in the cylindrical coordinate system in figure 4b there exists alignment of $\langle 100 \rangle$ directions with the radial direction, but no rotational symmetry around the radial direction due to the simultaneous alignment of $\langle 110 \rangle$ directions with the z-direction, i.e. the wire axis. The texture component representing a single orientation with $\langle 100 \rangle || r$ and $\langle 110 \rangle || z$ (a cube orientation rotated by 45° around r) in the cylindrical coordinate system translates to a cyclic $\{100\}\langle 110 \rangle$ fiber texture (denoting a tangential $\{100\}$ plane with its normal pointing radially outwards and one of the $\langle 100 \rangle$ directions along the z-axis.) Allowing a maximal disorientation angle of 15° between orientations and $\{100\}\langle 110 \rangle$, the volume fraction of this particular texture component becomes rather high (71 %).

Such a cyclic fiber texture, different from a cyclic ring fiber texture, has not been observed before in single fiber model composites; they always showed a cyclic $\langle 100 \rangle$ ring fiber texture, even in the absence of any oxide interlayer [9, 10]. Nevertheless, the reason for this specific texture occurring in the absence of an interlayer has to be linked to this absence establishing a direct interface between matrix and wire and the texture of the wire itself.

Orientations within the wire are revealed, if orientation maps are acquired with a smaller step size of 1 μm. As seen from the green color in the corresponding orientation map in figure 3.3a, a strong alignment of $\langle 110 \rangle$ directions with the wire axis (z-direction) occurs in the wire. The 110 pole figure in figure 6 obtained from orientations acquired only within the wire confirms this alignment. As exactly the same z-alignment is observed in the matrix of the model composite without any interlayer, it is proposed that the z-alignment of $\langle 110 \rangle$ directions is inherited from the texture of the wire, whereas the radial alignment of $\langle 100 \rangle$ directions is caused by growth during CVD. The presence of an yttria interlayer effectively hinders a potential transfer of the alignment in the wire to the growing matrix. It can reasonably be assumed that any undesired surface treatment of the wire before CVD will potentially disable such a transfer and that therefore only cyclic ring fiber textures have been observed before, but not cyclic fiber textures.

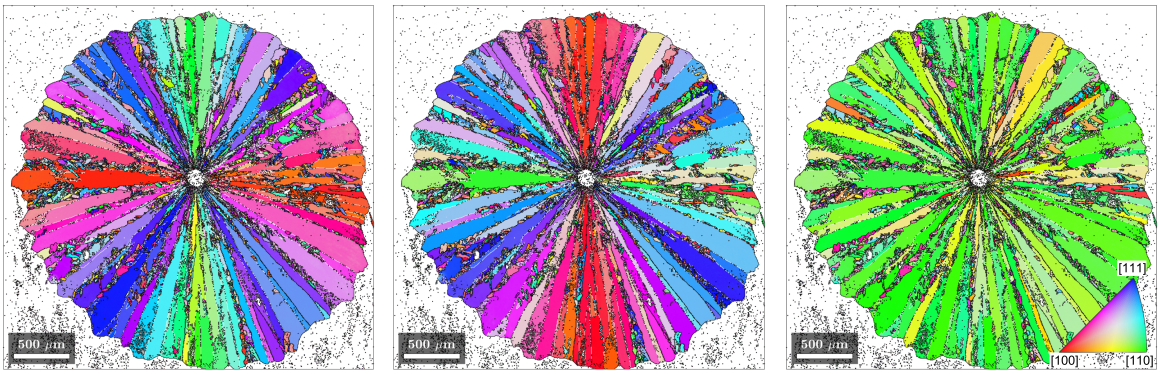

(a) (b) (c)

Figure 5. Orientation maps of the cross section of a single tungsten fiber-reinforced tungsten composite without an interlayer in the as-processed state. The colors reflect the crystallographic directions along different sample directions according to the inset: (a) along x-, (b) along y- and (c) along z-direction.

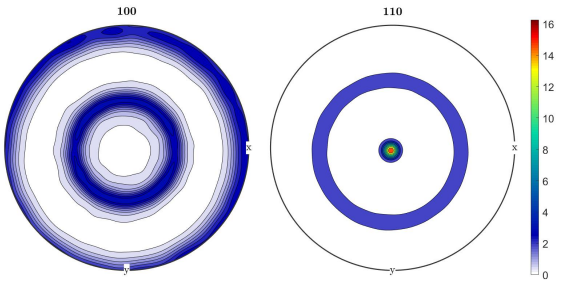

Figure 6. 100 and 110 pole figures obtained from orientation data acquired only within the wire on cross sections of single tungsten fiber-reinforced tungsten composites without any interlayer in the as-processed state. Pole densities are presented with respect to the directions of a Cartesian coordinate system (x,y,z) in stereographic projection.

3.3. Microstructural changes during annealing

Orientation maps obtained in the vicinity of the fiber on cross sections of single fiber composites with an 1 μm yttria interlayer and without an interlayer are collected in figures 3.3 and 3.3, respectively. The scale bars always represent the diameter of 150 μm of the original wires to facilitate comparison between the as-processed state and after annealing at 1450 °C for 4 hours or 2 weeks. In the as-processed state of both model composites, the drawn wire is easily identified: in case of the composite with interlayer (figure 3.3a) by the white ring of non-indexed points around the wire which indicates the yttria interlayer (the white ring appears thicker than 1 μm and uneven due to projection effects and the specimen inclination during EBSD), in case of the composite without any interlayer (figure 3.3a) by the abundant presence of high angle boundaries. In the matrix regions closest to the wire, a corona of many small, slightly elongated grains around the wire is observed; further out, wedge-shaped, columnar grains which eventually reach to the perimeter of the composites are revealed.

The microstructures after annealing at 1450 °C differ severely from those of the as-processed state highlighting the restoration processes taking place. In the composite with an interlayer (figure 3.3b), original position and perimeter of the wire can still be distinguished from the matrix after 4 days of annealing by its different microstructure (except a few locations). Grains just outside of the wire are larger than in the as-processed state and some grain growth must have taken place in the vicinity of the wire. Along the perimeter of the wire, the deformation structure is replaced by only a few large grains. Their different colors reveal orientations not dominantly present in the deformation structure. These newly formed grains extend from the perimeter of the wire towards its center. In the center of the wire, a region (revealed by green

(a) (b) (c)

Figure 7. Orientation maps of the central part (the wire and its neighborhood) of cross sections of single tungsten fiber-reinforced tungsten composites with a 1 μm thick yttria interlayer: (a) in the as-processed state, and after annealing at 1450 °C for (b) 4 days and (c) 2 weeks. The colors reflect the crystallographic directions along the z-direction according to the inset.

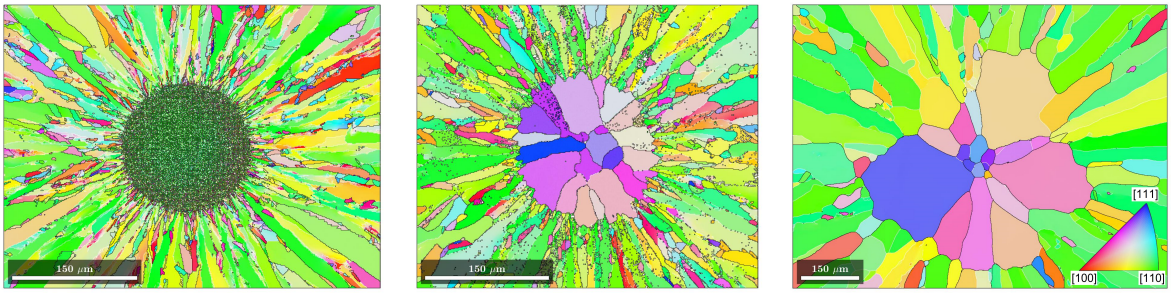

(a) (b) (c)

Figure 8. Orientation maps of the central part (the wire and its neighborhood) of cross sections of single tungsten fiber-reinforced tungsten composites without interlayer: (a) in the as-processed state and after annealing at 1450 °C for (b) 4 days and (c) 2 weeks. The colors reflect the crystallographic directions along the z-direction according to the inset.

color and many high angle boundaries) still exists where grains show an alignment of a ⟨110⟩ direction with the wire axis as for the deformation structure. The grains in the wire center appear slightly larger than the grains in the center of the wire in the as-processed state (figure 3.3a) indicating occurrence of recrystallization while preserving the texture. This changes entirely after 2 weeks of annealing (figure 3.3c) where the original position of the wire can almost not be recognized due to a region of at least 600 μm in diameter formed by huge grains larger than the original wire. The wire seems completely consumed by just two grains each about 80 μm big, while in the surrounding matrix, huge and only slightly elongated grains larger than 300 μm have developed.

While the yttria interlayer is clearly discerned in the as-processed state, this is not the case any longer after annealing. After two weeks at 1450 °C, only five small areas of non-indexed points exist revealing the presence of yttria (as confirmed by energy dispersive spectroscopy). After 4 days of annealing, despite the still obvious distinction between wire and matrix, just a few small areas with non-indexed points are observed along the perimeter of the wire. Apparently, the closed yttria interlayer has disintegrated and — driven by its phase boundary energy — spheroidized into single yttria particles along the original position of the layer.

After annealing of the model composite without interlayer for 4 days, a circular region with a diameter about 10 % larger than that of the wire is observed (figure 3.3b). Large grains (of about 50 μm) have replaced not only the deformation structure of the wire, but also parts of the matrix in the vicinity where quite small, slightly elongated grains are observed before annealing.

Significant grain growth in this circular region took place after recrystallization in the wire. The border between the circular region and the matrix shifted from the former interface between wire and matrix outwards; it appears quite corrugated adapting to the radially columnar grain structure of the matrix. After annealing for 2 weeks, huge grains have developed in a circular region with a diameter of about 500 μm, much larger than the diameter of the wire (figure 3.3c). The original location of the wire is presumed to be where a few relatively small grains (of about 30 μm) are seen. Huge grains grew radially with locally quite different progress; in some locations, further growth seems to be impeded by the columnar grains.

4. Conclusion

Tungsten fiber-reinforced tungsten composites with and without an yttria interlayer between fiber and matrix have been investigated. Model composites containing a single fiber have been produced by chemical vapor deposition of tungsten on a drawn tungsten wire. The microstructures in the as-processed samples and after annealing at 1450 °C for four days or two weeks were characterized by electron backscatter diffraction. Columnar grains and two different textures are revealed for the matrix in the as-processed state: the model composite with interlayer shows a cyclic $\langle 100 \rangle$ ring fiber texture from preferred growth, while the one without interlayer inherits additional axial alignment of $\langle 110 \rangle$ directions from the wire and develops a cyclic $\{100\}\langle 110 \rangle$ fiber texture. Such a heritage of preferred directions has not been observed so far in single fiber composites and is suggested to be caused by a different surface treatment of the wire before CVD. Substantial microstructural changes occur during annealing at 1450 °C: After four days of annealing, wire and matrix can still be discerned despite significant grain growth (following prior recrystallization in the fiber); after two weeks, the microstructures in the wire and in the matrix in the vicinity of the wire become (almost) indistinguishable independent of the presence or absence of an interlayer. Huge grains develop, the yttria interlayer disintegrates and only small yttria remnants can be traced at all. An yttria interlayer of 1 μm, unfortunately, proofs to be insufficient to prevent coupling between the restoration process in fiber and matrix at a temperature of 1450 °C.

Acknowledgments

This work has been carried out within the framework of the EUROfusion Consortium, funded by the European Union via the Euratom Research and Training Programme (Grant Agreement No 101052200 – EUROfusion). Views and opinions expressed are however those of the authors only and do not necessarily reflect those of the European Union or the European Commission. Neither the European Union nor the European Commission can be held responsible for them.

References

[1] Lassner E and Schubert W-D 1999 *Tungsten* (New York: Kluwer Academic) p 24
[2] Pintsuk G, 2012 *Compr. Nucl. Mater.* **4** 581
[3] Riesch J, Aumann M, Coenen JW, Gietl H, Holzner G, Höschen T, Huber P, Li M, Linsmeier C and Neu R 2016 *Nucl. Mater. Energy* **9** 83
[4] Gietl H, Riesch J, Coenen JW, Höschen T, Linsmeier C and Neu R 2017 *Fus. Eng. Des.* **124** 400
[5] Riesch J, Buffiere JY, Höschen T, Scheel M, Linsmeier C, and You JH 2018 *Nucl. Mater. Energy* **15** 12
[6] Schade P 2002 *Int. J. Refr. Met. Hard Mater.* **54** 351
[7] Riesch J, Han Y, Almanstötter J, Coenen JW, Höschen T, Jasper B, Zhao P, Linsmeier C and Neu R 2016 *Physica Scripta* **T167** 014006
[8] Mao Y *et al.* 2019 *Nucl. Fusion* **59** 086034
[9] Ciucani UM, Haus L, Gietl H, Riesch J and Pantleon W 2021 *J. Nucl. Mater.* **543** 152579
[10] Ciucani UM, Haus L, Gietl H, Riesch J and Pantleon W 2021 *IOP Conf. Ser.: Mater. Sci. Eng.* **1121** 012024
[11] Bachmann F, Hielscher R and Schaeben H 2011, *Solid State Phenom.* **160** 63
[12] Pantleon K, Jensen JAD and Somers MAJ 2008 *J. Electrochem. Soc.* **151** 45
[13] Wassermann G and Grewen J 1962 *Texturen metallischer Werkstoffe* 2nd ed. (Berlin: Springer Verlag) p 7